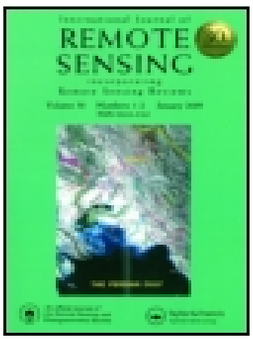

International Journal of Remote Sensing

ISSN: 0143-1161 (Print) 1366-5901 (Online) Journal homepage: https://www.tandfonline.com/loi/tres20

Satellite remote sensing of primary production

C. J. TUCKER & P. J. SELLERS

To cite this article: C. J. TUCKER & P. J. SELLERS (1986) Satellite remote sensing of primary production, International Journal of Remote Sensing, 7:11, 1395-1416, DOI: 10.1080/01431168608948944

To link to this article: https://doi.org/10.1080/01431168608948944

Published online: 27 Apr 2007.

INT. J. REMOTE SENSING, 1986, VOL. 7, NO. 11, 1395–1416

Satellite remote sensing of primary production

C. J. TUCKER and P. J. SELLERS

Earth Resources Branch, Code 623, NASA/Goddard Space Flight Center, Greenbelt, Maryland 20771, U.S.A.

Abstract. Leaf structure and function are shown to result in distinctive variations in the absorption and reflection of solar radiation from plant canopies. The leaf properties that determine the radiation-interception characteristics of plant canopies are directly linked to photosynthesis, stomatal resistance and evapotranspiration and can be inferred from measurements of reflected solar energy. The effects of off-nadir viewing and atmospheric constituents, coupled with the need to measure changing surface conditions, emphasize the need for multitemporal measurements of reflected radiation if primary production is to be estimated.

1. Introduction

Photosynthesis in terrestrial vegetation occurs in chloroplast organelles, which are largely contained within plant leaves. The reaction process of photosynthesis can be summarized as $CO_2 + H_2O \rightarrow$(light energy)$\rightarrow [CH_2O] + O_2$, where CO_2 and H_2O are combined, driven by light absorption to produce carbohydrates, and release O_2. Consequently, the structure of leaves is highly evolved to facilitate photosynthesis. Leaf structure allows for regulated contact between the atmosphere, which is the source for the CO_2, and the hydrated mesophyll cells, which contain the water required, while maintaining an optical environment in which incident photosynthetically active radiation (0·4–0·7 μm) can interact with the chloroplast-containing cells where photosynthesis takes place (figure 1).

2. Spectral properties of vegetation

One of the first observations of intraleaf structure is the labyrinth of intercellular air spaces. This air-filled labyrinth brings the air with its fractional CO_2 content into direct contact with the chloroplasts, permitting absorption of CO_2 and liberation of O_2. Air enters and exits leaves through stomata in the upper and lower epidermal surfaces. H_2O is present within the hydrated interior of mesophyll cells, and is thus available to the chloroplasts. Photosynthetically active radiation (PAR) (0·4–0·7 μm) is able to penetrate the upper epidermal surface of leaves, which are largely transparent to incident PAR (Willstaetter and Stoll 1918, Gates *et al.* 1965, Knipling 1970, Woolley 1971, Gausman 1974). Only 2–3 per cent of the PAR of normal incidence is initially reflected by the upper epidermal surface, the balance being transmitted into the interior of the leaf. As the incident PAR flux enters the leaf it becomes increasingly scattered or deflected as a consequence of reflective–refractive and Rayleigh/Mie scattering (Gates *et al.* 1965, Allen *et al.* 1969, 1970, 1971).

Rayleigh scattering occurs for particles of sizes equal to or less than the wavelength of the incident radiation, and is proportional to the inverse fourth power of the wavelength. While organelles such as chloroplasts, for example, are 4–6 μm in length and 1–2 μm thick, other organelles such as lysosomes and macromolecules such as proteins, lipids, and carbohydrates can be smaller than 1 μm and would cause Rayleigh

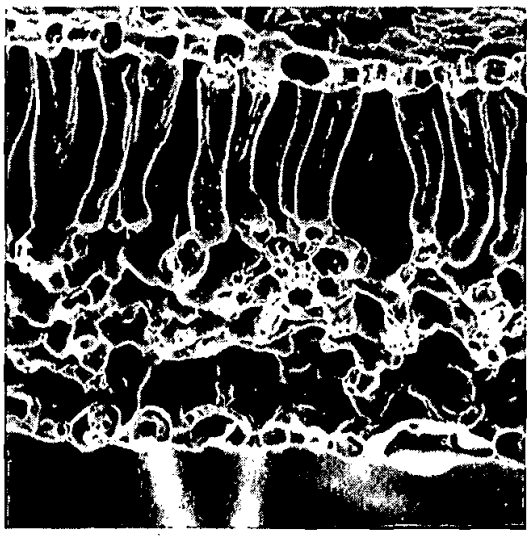

Figure 1. Transverse section of a broad-bean leaf. Beneath the upper epidermis is a layer of elongated palisade parenchyma cells. The lower half of the leaf contains the spongy mesophyll. Also note the labyrinth of the intercellular air spaces.

scattering. J. T. Woolley (1976 personal communication) has estimated that only about 10 per cent or less of the internal leaf scattering is due to Rayleigh scattering and that this is largely due to small refractive-index discontinuities among the intercellular constituents.

The main cause of scattering within leaves is refractive–reflective scattering, which occurs as a consequence of the refractive-index differences between intercellular air spaces (1·0) and hydrated cells (1·4) and the irregular facets of the exteriors of cells (figure 1). As incident solar radiation in the 0·4–2·5 μm region enters the leaf and penetrates downward, it becomes increasingly scattered from the combination of internal cellular reflections and the air–cell refractive-index differences.

PAR is absorbed strongly within green leaves by the plant pigments present. Most of this absorption is due to chlorophyll a, chlorophyll b, and the carotenoids (Salisbury and Ross 1969). The absorption of incident solar radiation by plant pigments and liquid water can be described by the Lambert–Beer exponential extinction law.

The relative proportion of the plant pigments varies; the chlorophylls usually make up 60–75 per cent, the carotenoids 25–35 per cent, and the other minor pigments the balance. The chlorophylls and carotenoids account for the great majority of total leaf-pigment absorption. Liquid water is also present in leaf tissues, comprising 70–90 per cent of the wet weight of leaves. While liquid water is transparent to the PAR wavelengths, it is a strong absorber in the 1·3–2·5 μm region (Curcio and Petty 1951). The coefficients of absorptance for chlorophyll a, chlorophyll b, the carotenoid lutein, and liquid water are presented in figure 2.

The interaction of incident solar radiation in the 0·4–2·5 μm region with green leaves has been modelled using ray-tracing models (Allen *et al.* 1973, Kumar and Silva 1973) and by a stochastic Markov-chain model (Tucker and Garrett 1977). To generate these models, scattering and absorption properties were required. Scattering by the structures within leaves has the effect of increasing the mean pathlength of the incident

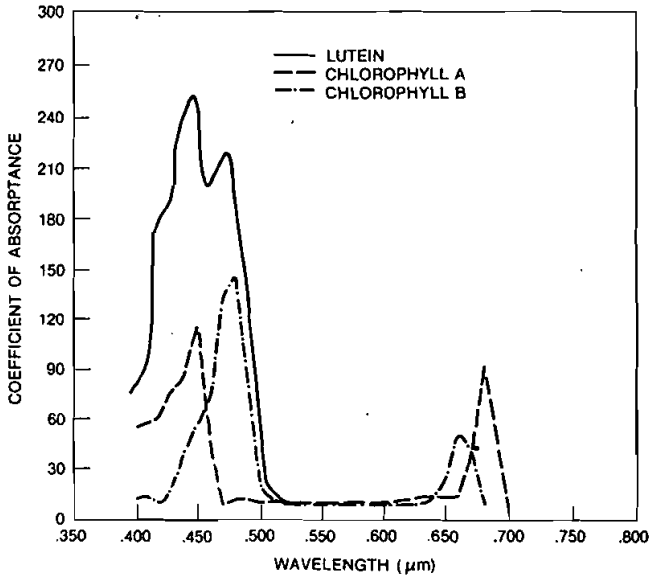

(*a*)

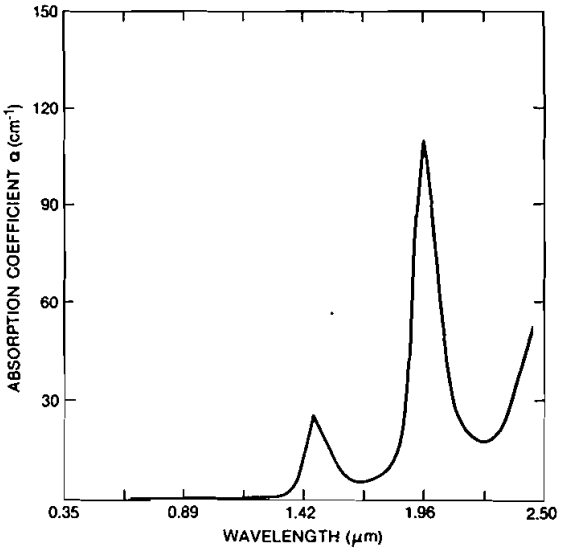

(*b*)

Figure 2. Coefficients of absorptance for chlorophyll a, chlorophyll b, and lutein (*a*) and pure liquid water (*b*).

PAR, thereby allowing for high levels of PAR absorption by the photosynthetic pigments. The same scattering mechanisms necessary for photosynthesis result in high values of leaf reflectance in the 0·7–1·3 μm region where little absorption occurs (figure 2). In the absence of absorption, the scattering mechanisms enhance the back-scattered radiation more than the forward-scattered radiation.

When incident solar radiation interacts with functioning green leaves there is a high level of absorption in the PAR (0·4–0·7 μm) region and corresponding low values for reflectance and transmittance. In the 0·7–1·3 μm region, because of very low absorption, there is high reflectance and transmittance. Higher absorption levels of absorption in the 1·3–2·5 μm region result in lower values for reflectance and transmittance. The ratios of the absorbed, reflected and transmitted radiation to the incident solar irradiance at the same wavelength are referred to as the spectral absorption, spectral reflection and spectral transmittance respectively, to denote that these are functions of wavelength.

While the incident spectral irradiance that interacts with green leaves results in absorbed, reflected and transmitted radiances as functions of wavelength, the same interaction with plant canopies results in only spectral absorption or spectral reflection. Spectral transmittance is an intermediate state, which ultimately is absorbed and/or reflected within the plant canopy and/or by the background material. The spectral radiance from plant canopies in the 0·4–2·5 μm region provides the basis for passive remote sensing of vegetated areas and can be measured from ground, airborne and spaceborne sensors.

The *in situ* plant-canopy reflectance variability introduced by different soil backgrounds has been reported to vary substantially between dark and very light soils for a variety of vegetation covers (Colwell 1974, Erza *et al.* 1984, Huerte *et al.* 1984, 1985, Elvidge and Lyon 1985). This is usually more pronounced for sparse canopies than for more heavily vegetated areas. Huerte *et al.* (1984, 1985) have reported that the variability of the soil background reflectance has a strong effect on all the 'greenness' indices, concluding that the only solution for overcoming this was to have accurate information on the soil spectral reflectivities for the soils encountered in areas that were being studied by remote-sensing methods.

Remote-sensing studies of vegetation normally use specific wavelengths selected to provide information about the vegetation present in the area from which the radiance data emanated. These wavelength regions are selected because they provide a strong signal from the vegetation and also have a spectral contrast from most background materials. The primary consideration in sensor wavelength selection is that a strong green-vegetation–background-material reflectance difference must occur. Without a strong spectral contrast, vegetation-canopy information is degraded or confused with non-vegetation information. This can be schematically represented in a simplistic sense by overplotting vegetation spectral reflectance with that from a typical soil (figure 3).

Five primary and two transition regions have been proposed between 0·4–2·5 μm, where differences in leaf optical properties (scattering and absorption) and the background optical properties control plant-canopy spectral reflectance (Tucker 1978; figure 3). These seven regions are slightly modified by differences in the background material present, density of the plant canopy (i.e. more for sparse canopies, less for full canopies, etc.), solar zenith angle and sensor view angle. The regions are: (1) 0·4–0·5 μm, where strong spectral absorption by the chlorophylls and carotenoids occurs; (2) 0·5–0·62 μm, where reduced levels of chlorophyll absorption occur (i.e. why green vegetation to our eyes appears 'green'); (3) 0·62–0·7 μm, where strong chlorophyll absorption occurs (see figure 2*a*); (4) 0·70–0·74 μm, where strong absorption ceases; (5) 0·74–1·1 μm, where minimal absorption occurs and the leaf scattering mechanisms result in high levels of spectral reflectance, especially for dense canopies; (6) 1·1–1·3 μm, where the liquid-water coefficients of absorption increase from close to 0 at 1·1 μm to values of 4 at 1·3 μm; and (7) 1·3–2·5 μm, where absorption by liquid

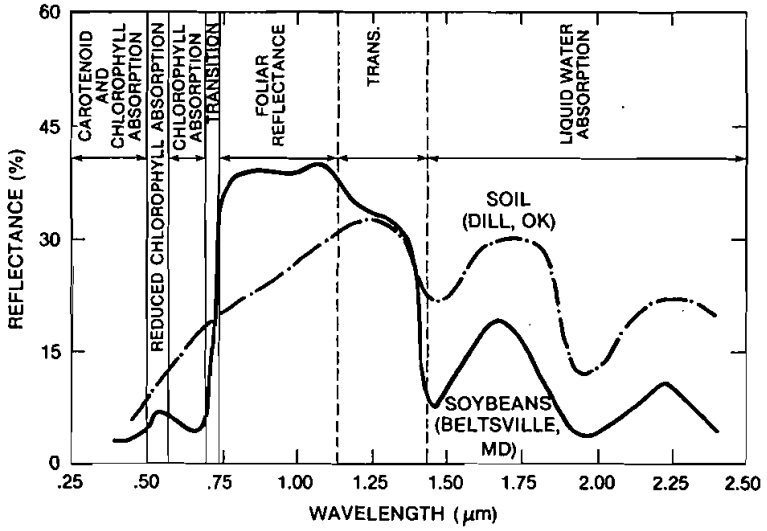

Figure 3. Delineation of the 0·4–2·5 μm region into spectral intervals where different biophysical properties of green vegetation control the reflectance of incident solar irradiance from the vegetation in question. Sample spectral reflectance curves for green vegetation and soil are also included to illustrate why some wavelengths have greater spectral contrasts than others.

water occurs (figure 2*b*). It should also be understood that background-material reflectance differences can increase or decrease spectral contrasts and hence shift these general intervals somewhat (Colwell 1974, Erza *et al.* 1984, Huerte *et al.* 1984, 1985, Elvidge and Lyon 1985).

Information about vegetation canopies, potentially available from the 0·4–0·7, 0·74–1·1 and 1·3–2·5 μm regions, is related respectively to the plant pigments present, the projected green-leaf density and the liquid water present. Within the 0·4–0·7 μm region, the strongest spectral contrast usually occurs in the 0·62–0·68 μm zone, this being the wavelength region usually employed to infer the degree of *in situ* chlorophyll absorption in plant canopies. The subinterval of the 0·74–1·1 μm region is usually chosen for inferring projected green-leaf reflectance. The desire to avoid atmospheric water-vapour absorption bands usually results in the selection of the 0·79–0·90 μm spectral interval within the 0·74–1·1 μm interval. The subinterval(s) usually selected for use in inferring liquid-water absorption within plant canopies in the 1·3–2·5 μm interval is also based upon the consideration of avoiding atmospheric water-vapour absorption within this spectral interval while maintaining a spectral contrast between the background material and canopy leaf water content. This results in the 1·55–1·75 and 2·1–2·3 μm spectral intervals being selected (Tucker 1980).

Remote-sensing studies of vegetation can thus use spectral-radiance data from the 0·4–0·7, 0·74–1·1 and 1·3–2·5 μm regions to infer properties related to pigment absorption, the projected green leaf density, and the canopy leaf water content. However, the pigment absorption is highly coupled with the canopy leaf water content, and thus satellite remote sensing of vegetation has usually used two wavelength regions to infer biophysical properties of plant canopies. These two regions are the upper portion of the visible (i.e. 0·6–0·7 μm) and the near-infrared (0·75–1·1 μm). Satellite measurements using these two wavelength regions can be ratioed or combined to normalize differences in solar spectral irradiance while providing nondestructive

spectral information about the degree of absorption and scattering that occur within the area from which the satellite-measured radiances emanated.

We have discussed the relationships between leaf structure and function and how these determine the spectral reflectance characteristics of plant canopies. It is these relationships that are used to infer characteristics of plant canopies using measurements of reflected radiation made by satellites. Several companion papers in this issue report on the use of satellite data for studying African vegetation. These satellite-measured spectral radiances are also influenced by variable sun–target–sensor geometry and by the composition of the atmosphere through which the sensing occurs.

The effects of solar zenith angle upon spectral data have been reported by Duggin (1977) and Kimes *et al.* (1980). Kimes (1983, 1984) and Kimes *et al.* (1984) have reported that surface spectral reflectances in the 0·55–0·68 and 0·73–1·1 μm bands from complete homogenous plant canopies at all sun angles tended to a minimum near nadir and showed increasing spectral reflectance with increasing off-nadir viewing for all azimuth directions. In some cases, the minimum spectral reflectance was shifted slightly off-nadir in the forward-scattering direction. In all complete homogenous canopy cases, the spectral-reflectance distributions tended to be azimuthally symmetric. For sparse vegetation canopies, the anisotropic scattering properties of the soil significantly influenced the directional spectral reflectance. This results from the fact that soil spectral reflectance has a strong backscattering characteristic that can dominate observed reflectance distributions for sparse canopies under lower solar zenith angles.

Measurements of solar reflected radiation from satellites also include varying degrees of atmospheric influence. In this paper, because we are interested in using visible and near-infrared wavelength radiation to infer estimates of primary production, we will confine our discussion to these specific wavelength regions. Satellite estimates of primary production usually involve the use of the 'greenness' indices. These are various combinations of visible and near-infrared radiation (Tucker 1980, Curran 1983, Jackson 1983, Perry and Lautenschlager 1984). Holben and Fraser (1984) and Fraser and Kaufman (1985) have reported on the effects of atmospheric scattering and absorption upon radiation in these wavelength regions. It has been reported that, except under twilight conditions, factors such as off-nadir viewing, atmospheric aerosol scattering and clouds can only decrease 'greenness' indices. This has resulted in the method of obtaining daily satellite data, mapping it to a common coordinate system, verifying the geographic registration of the mapped data, and then selecting the highest 'greenness' value over a several-day period (Holben, 1986). Not only does this minimize the effects of sun–target–sensor geometry and the atmosphere, but it also provides the necessary data to follow vegetation 'greenness' or the photosynthetic capacity through time.

3. Chlorophyll density and leaf physiology

The first part of this paper has discussed how green vegetation preferentially absorbs visible radiation or photosynthetically active radiation (PAR, 0·4–0·7 μm), and uses this harvested energy to drive the exothermic photosynthetic reaction. This fact helps the would-be remote sensor enormously, as the presence or absence of green vegetation and, by inference, photosynthesis and transpiration, are distinctively marked by the unusual spectral properties of green leaves. Put another way, it is relatively easy to apply remote-sensing techniques to the detection of a process that has a strong radiative-transfer component associated with it.

A review of the spectral properties of green leaves allows us to specify the likely products and limitations of remote-sensing applications in the particular case of terrestrial vegetation: clearly, the direct result of red and near-infrared remote-sensing observations will be some indication of the surface chlorophyll density. Since this quantity is related to the rate at which the plant cover can fix carbon dioxide and water into carbohydrates, these observations should yield information about the photosynthetic capacity of the vegetated surface. In this context, the term 'photosynthetic capacity' means the gross photosynthetic rate of the canopy under specified illumination conditions assuming no sources of environmental stress; for example, soil moisture deficit or extremes of temperature. The photosynthetic capacity therefore specifies the upper limit of the photosynthetic rate for a given PAR flux. This definition may seem unnecessarily pedantic, but it is entirely justified: simply observing the surface chlorophyll density at a given instant only provides information about the *maximum* photosynthetic output of the system. The *actual* rate of photosynthesis at the time will be determined by the PAR flux, moisture availability, etc. An indication of the photosynthetic capacity immediately leads to correlative information about the minimum canopy resistance. The atmospheric carbon dioxide used in photosynthesis diffuses into the leaves via the stomatal pores, and, at the same time, water vapour diffuses out of the leaf's saturated interior via the same route (figure 4). Most terrestrial plants may experience soil moisture stress from time to time, and they generally control the width of their stomatal apertures in such a way that photosynthesis of CO_2 influx is maximized and transpired water or H_2O efflux is minimized (Farquhar and Sharkey 1982, Williams 1983). This may be expressed mathematically as

$$dP/dE = W \tag{1}$$

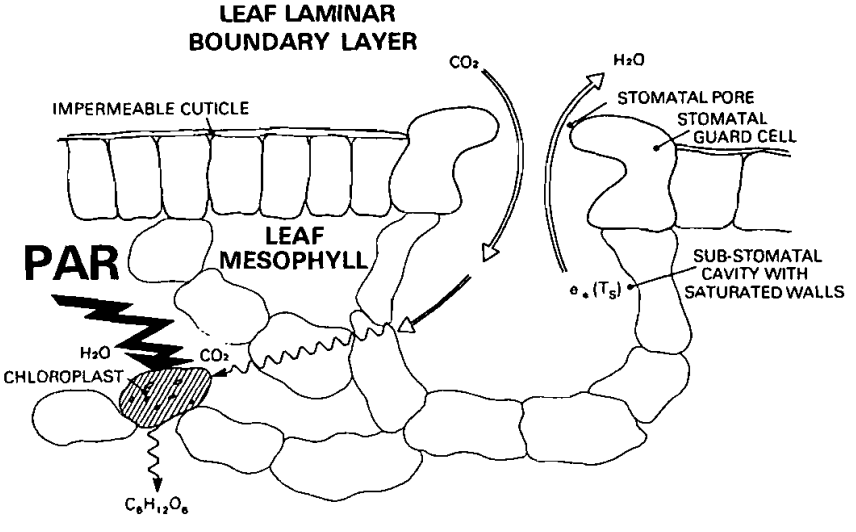

Figure 4. Schematic diagram showing passage of CO_2 and water vapour in and out of plant leaves. The photosynthetic reaction takes place in the light-trapping organelles, the chloroplasts, while gas exchange is regulated by the aperture of the stomatal guard cells (see also figure 1).

where P is the photosynthetic rate (in kg/m^2/s), E is the transpiration rate (in kg/m^2/s) and W is the constant of water-use efficiency. The leaf gross photosynthetic rate, P is normally described by

$$P=\frac{a_1 F_\downarrow}{b_1+F_\downarrow}-R_d \tag{2}$$

a_1 is a constant (in kg/m^2/s), b_1 is a constant (in W/m^2), $F_\downarrow$ is the normal incident flux of PAR (in W/m^2) and R_d is the dark respiration rate (in kg/m^2/s). This is a convenient form, which is relatively easy to fit to data. Theoretical work by Farquhar and von Caemmerer (1982) predicts a response of P to increasing PAR flux similar to equation (2). From equation (2) we see that for low PAR fluxes, P is almost linearly related to $F_\downarrow$, the gradient of the relationship being given by a_1/b_1, as initially the photosynthetic system is limited by the amount of available energy. At saturating PAR fluxes, P approaches an asymptote, defined by the value of a_1, as the amount of the leaf's capital of photosynthetic machinery (principally the carboxylating enzymes) becomes the limiting factor. The amount of chlorophyll in the leaf will also influence the overall relationship between P and the PAR flux.

The application of equation (1) for water-use efficiency and an assumption of a more or less constant leaf mesophyll concentration of CO_2 implies that the light-dependent part of stomatal functioning should follow the leaf photosynthetic response closely. We can describe the flux of CO_2 from the atmosphere to the leaf interior by the potential difference of the CO_2 concentration gradient, C_a-C_i, and the diffusion impedance of the stomatal pores, r_s. We then have, under steady-state conditions,

$$J=\frac{C_a-C_i}{1{\cdot}6r_s} \tag{3}$$

where J is the CO_2 flux (in kg/m^2/s), C_i is the substomatal CO_2 concentration (in kg/m^3), C_a is the atmospheric CO_2 concentration (in kg/m^3), r_s is the stomatal resistance to water-vapour transfer (in s/m) and 1·6 is a factor that accounts for the different diffusivities of CO_2 and water vapour in air. The transpiration rate from the saturated substomatal cavity may be written as

$$E=\frac{(e^*(T)-e_a)}{r_s}\frac{\rho c_p}{L\gamma} \tag{4}$$

where E is the transpiration rate (in kg/m^2/s), $e^*(T)$ is the saturated vapour pressure (in mb) at temperature T, e_a is the vapour pressure (in mb) outside the leaf surface, ρ, c_p are the density and specific heat of air (in kg/m^3 and J kg^{-1} K^{-1} respectively), L is the latent heat of vaporization (in J/kg) and γ is the psychrometric constant (in mb/K). Here the potential difference is made up from the differences in water-vapour pressure in the leaf, which is saturated, and in the free air. Since, under steady-state conditions, the influx of CO_2, J must satisfy the demands of the photosynthetic rate P by the equality

$$J=1{\cdot}375\,P \tag{5}$$

where 1·375 is the ratio of molecular weights of six CO_2 molecules to one basic glucose molecule ($=(6\times 44)/192$), we may combine equations (3) and (5) and then equation (2)

to give an equation for the expected behaviour of r_s:

$$r_s = \frac{\Delta C}{1{\cdot}6 \times 1{\cdot}375} \frac{1}{P} \quad (\text{where } \Delta C = C_a - C_i) \tag{6}$$

$$= \frac{\Delta C}{1{\cdot}6 \times 1{\cdot}375} \left[\frac{b_1 + F_\downarrow}{a_1 F - R_d(b_1 + F_\downarrow)} \right]$$

For small values of the dark respiration term R_d this becomes

$$r_s = a_2/F_\downarrow + c_2$$

where the values of a_2 and c_2 may be recovered from equation (6). Normally r_s is expressed slightly differently (Jarvis 1976) as

$$r_s = \frac{a_2}{b_2 + F_\downarrow} + c_2 \tag{7}$$

where a_2, b_2 and c_2 are species-dependent constants (in J/m^3, W/m^2 and s/m respectively) and are obtained from fits to data. Figure 5 shows typical leaf photosynthesis and transpiration-resistance responses for maize leaves.

To sum up the discussion so far, the local density of chlorophyll, which is quantifiable from remote-sensing measurements, is an indicator of the photosynthetic capacity of the plant canopy. Moreover, because of the strong links between photosynthesis and transpiration, the chlorophyll density is also an indicator of the minimum stomatal resistance of the vegetation to water-vapour transfer. Additional information about the type of vegetation being observed (which will determine the values of a_1, b_1, a_2, b_2, and c_2 and R_d) and the local forcings (PAR flux, soil moisture, temperature, etc.) allows the actual photosynthetic rate and canopy stomatal resistance to be estimated. It is clear from the above that the remotely sensed estimates of chlorophyll density provide us with information about rates associated with the vegetation (photosynthesis, transpiration) rather than a given state of the surface (leaf-area index or biomass). In the rest of this section this point will be expanded with the aid of simple mathematical models that place the preceding qualitative statements in a physical context.

Up to now, we have discussed the remote-sensing problem in terms of an abstract quantity, the chlorophyll density. Clearly, if we were in the position of detecting thin flat isotropic chlorophyllous particles scattered on a uniform background and arranged without any mutual overlapping (and hence no radiative interaction) the remote-sensing inversion problem would be fairly straightforward. Unfortunately, the real world is not so accommodating. The main complication presented by reality is that the chlorophyll-bearing phytoelements, leaves or needles, are usually distributed throughout a canopy volume, as opposed to lying directly on the background surface; they are usually arranged with a variety of angular orientations, as opposed to being horizontal plates; and they frequently possess more than a unit of total projected area per unit of underlying surface area (the leaf area index exceeds 1·0). To make things worse, canopy optical properties range from the nearly isotropic to relatively anisotropic, depending on species and health, and the local heterogeneity of the canopy density can be fairly extreme, as in the case of coniferous trees, where the needles are clustered into shoots. A full description of the radiative-transfer process in the more complex situations that nature can offer is beyond the capabilities of simple analytical techniques, requiring the application of numerical ray-tracing models or Monte Carlo

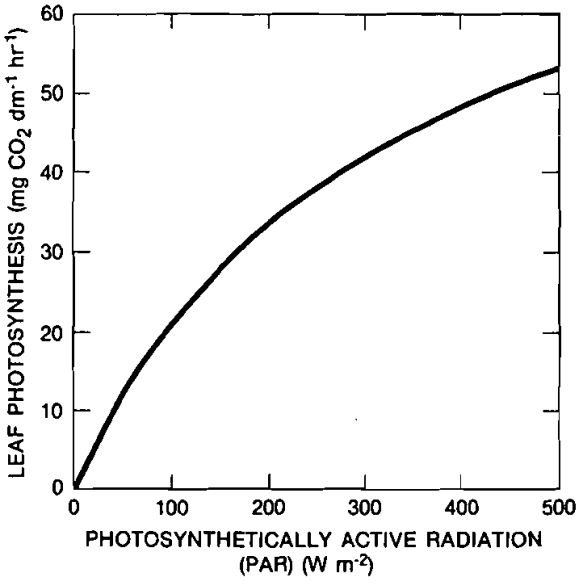

(*a*)

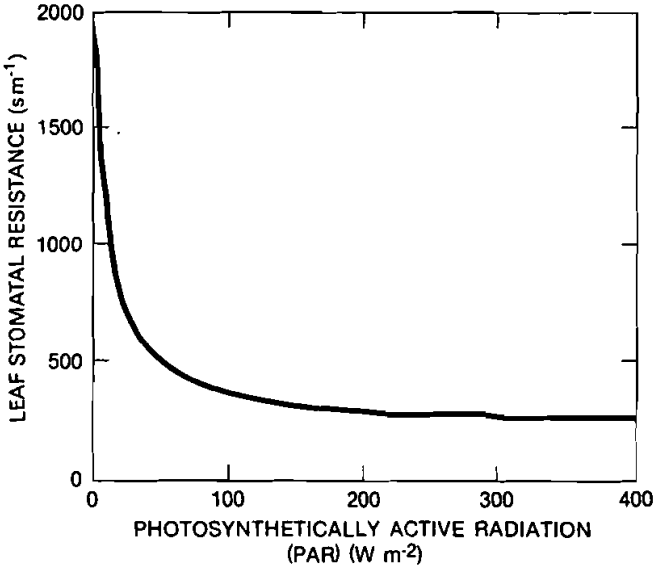

(*b*)

Figure 5. (*a*) Photosynthetic response of a maize leaf with increasing photosynthetically active radiation (PAR) absorbed (fitted to data from Hesketh and Barker 1967). (*b*) Transpiration resistance of a maize leaf as a function of increasing PAR absorbed (fitted to data from Turner 1974).

methods. Such methods are computationally expensive to apply, and unless used carefully may be fairly opaque to the user as to the causality of specific results. Additionally, such models require a large number of input parameters, the exact specification of which may be difficult to provide. On the other hand, these models can be instructive about the importance of particular parameters, and may be used to calculate the angular field of the reflected radiation, an essential requirement for comparisons with observations from remote-sensing instruments, which usually have a narrow field of view. For the purpose of illustration, we shall discuss a simple analytical model that allows us more direct physical insight into the remote-sensing problem and helps us to prioritize field-data needs on the basis of simple sensitivity analyses. We shall use such a model to describe the process of radiative transfer in plant canopies and a modification of the same model to calculate the attenuation and utilization of PAR within the distributed canopy. The outcome of this analysis is an insight into the relationships linking canopy reflectances, photosynthetic capacities and minimum resistances.

4. Canopy models of radiative transfer, photosynthesis and stomatal resistance

The radiative-transfer model to be used is the two-stream approximation described by Ross (1975), Meador and Weaver (1980), Dickinson (1983) and Sellers (1985) for applications in plant canopies. In this model, the intensity of diffuse radiation within the canopy is described by two differential equations, the first (8) defines the variation of the upward (integrated over the upper hemispherical directions) diffuse flux; the second (9) defines the equivalent downward diffuse flux:

$$-\bar{\mu}\frac{dI^{\uparrow}}{dL}+(1-(1-\beta)\omega)I^{\uparrow}-\omega\beta I_{\downarrow}=\omega\bar{\mu}K\beta_0\exp(-KL) \tag{8}$$

$$\bar{\mu}\frac{dI^{\uparrow}}{dL}+(1-(1-\beta)\omega)I_{\downarrow}-\omega\beta I_{\uparrow}=\omega\bar{\mu}K(1-\beta_0)\exp(-KL) \tag{9}$$

where $I_{\uparrow}$, $I_{\downarrow}$ are the upward, downward diffuse radiative fluxes, integrated over their respective hemispheres, $K=G(\mu)/\mu$ is the optical depth of direct beam per unit leaf area, $G(\mu)$ is the projected area per unit leaf area in direction $\cos^{-1}(\mu)$, μ is the cosine of zenith angle of incidence of direct beam radiation, $\bar{\mu}=\int_0^1(\mu'/G(\mu'))\,d\mu'$ is the average inverse diffuse optical depth per unit leaf area, ω is the scattering coefficient of leaves, μ' is the cosine of the angle of scattered flux, β, β_0 are the upscatter parameters of the diffuse and direct beams respectively, and L is the cumulative leaf-area index. Physical processes can be assigned to each of the terms in equations (8) and (9). Equation (8) describes the vertical profile of the upward diffuse radiative flux: the first term in (8) describes the attenuation of the flux, the second term defines that fraction of $I_{\uparrow}$ that is rescattered in an upward direction following interception with the leaves; the third term defines the fraction of the downward diffuse flux $I_{\downarrow}$ that is intercepted and scattered into the upward hemisphere to contribute to $I_{\uparrow}$, and the last term, on the right-hand side of (8), refers to the contribution to the upward diffuse flux by the scattering of the direct incident flux intercepted at the specified level L in the canopy. Corresponding descriptions may be assigned to the four terms in equation (9) that describe the profile of the downward diffuse flux. This model is simplistic in that it specifies only two possible directions for the scattered diffuse flux: upward and downward. In reality, and in the more complex numerical models, the scattered flux may be assigned to any number of directions. Nonetheless, the two-stream model does

take some account of the multiple-scattering process and in comparisons with a numerical model (see Kimes and Sellers 1985), the simplifications inherent in the two-stream model do not seem to give rise to serious errors.

Equations (8) and (9) may be solved analytically provided we have the means of specifying the various optical parameters $\bar{\mu}$, K, β and β_0. The specification of $\bar{\mu}$ and K is straightforward: $\bar{\mu}$ is commonly close to unity while K is equal to $G(\mu)/\mu$. The scattering parameters β and β_0 are more complicated, depending on the leaf-angle distribution and the values of the leaf reflectance and transmission coefficients. Methods for calculating the values of the coefficients for a number of simple cases are explained in some detail in Sellers (1985) and Dickinson (1983). In this paper we shall confine ourselves to the simplest possible case, that of a canopy with horizontal leaves, in which case $\bar{\mu}$ and K are both equal to 1, and β and β_0 are equal to 0·5 (which amounts to saying that half of the scattered flux goes upwards and half goes downwards). Suitable boundary conditions may then be applied to equations (8) and (9) to solve the set for a given radiational forcing. For an incident direct beam flux, the boundary conditions are as follows.

For the case of incident direct flux only,

$$I_{\downarrow}=0, \quad L=0 \tag{10}$$

$$I_{\uparrow}=\rho_s(\exp(-KL_t)+I_{\downarrow}), \quad L=L_t \tag{11}$$

where L_t is the total leaf-area index. The first condition simply states that at the top of the canopy ($L=0$) there is no downward diffuse flux; the second condition states that beneath the canopy (i.e. when $L=L_t$, L_t being the total leaf-area index), the upward diffuse flux is equal to the reflected portion of the total downward flux at $L=L_t$, which is the sum of the direct flux that gets through the canopy, $\exp(-KL_t)$, and the downward-scattered diffuse flux at the same level, $I_{\downarrow}$, multiplied by the soil surface reflectance ρ_s.

For the case of incident diffuse fluxes only,

$$I_{\downarrow}=1, \quad L=0 \tag{12}$$

$$I_{\uparrow}=\rho_s I_{\downarrow}, \quad L=L_t \tag{13}$$

and the direct-beam terms on the right-hand sides of equations (8) and (9) are replaced by zeros.

Solution of equations (8) and (9), using the specified coefficients and boundary conditions, yields two explicit equations for the upward and downward diffuse fluxes within the canopy. These have the form

$$I_{\uparrow}=\frac{h_1}{\sigma}\exp(-KL)+h_2\exp(-hL)+h_3\exp(hL) \tag{14}$$

$$I_{\downarrow}=\frac{h_4}{\sigma}\exp(-KL)+h_5\exp(-hL)+h_6\exp(hL) \tag{15}$$

where the constants $h_1, \ldots, h_6, h$ and σ are all albegraic combinations of the coefficients in equations (8) and (9), and in the boundary conditions. The reflectance of the vegetated surface is then given as the upward diffuse flux at $L=0$:

$$\begin{aligned} a&=I_{\uparrow}, \quad L=0 \\ &=\frac{h_1}{\sigma}+h_2+h_3 \end{aligned} \tag{16}$$

where a is the hemispherically integrated reflectance. The full expressions for the various constants in equations (14) and (15) are given in Sellers (1985). For our case of horizontal leaves, the equation set yields the same answer regardless of the direction of the incoming flux. In this case, equation (16) may be simplified to

$$I_\uparrow(L=0)=a=\frac{\omega(1-A)}{2(p_1-p_2A)} \tag{17}$$

where

$$A=\frac{p_1-\gamma}{p_2-\gamma}\exp(-2hL_t)$$

ω is the leaf scattering coefficient and is equal to the leaf reflectance plus transmittance,

$$p_1=1-\tfrac{1}{2}\omega+h, \quad p_2=1-\tfrac{1}{2}\omega-h$$

$$h=(1-\omega)^{1/2}, \quad \gamma=\omega/2\rho_s$$

Equation (17) is worth some closer study. The composite terms are all functions of the leaf scattering coefficient ω, except for A, which is a function of ω, the soil surface reflectance, ρ_s and a term which translates to the negative exponent of twice the diffuse optical pathlength of the canopy, $\exp(-2hL_t)$. A is the term that determines the relative contributions of the soil and the vegetation to the total reflectance, and this is dependent upon the attentuation of radiation going down and through the canopy (equivalent to one times $\exp(-hL_t)$), reflected from the soil surface and then transmitted back up through the canopy (which amounts to another $\exp(hL_t)$ term) hence giving rise to the factor 2 in the $\exp(-hL_t)$ term.

If we accept that the two-stream model provides us with a reasonable representation of how the vegetated surface absorbs and reflects the incident radiation, we may obtain an expression for the dependence of the canopy reflectance on leaf area index by simply differentiating equation (17) with respect to L_t to give

$$\frac{da}{dL_t}=\omega hA\frac{p_1-p_2}{p_1-p_2A} \tag{18}$$

Now for most field conditions where vegetation is found for significant portions of the year, the soil reflectance is low owing to the amount of organic matter present in the upper layers. This being so, the p_2A terms in equations (17) and (18) are relatively small, and we find that for the near-infrared (NIR) wavelength interval,

$$\frac{da_N}{dL_t}\propto A_N\exp(-2h_NL_t) \tag{19}$$

a_N is the near-infrared surface reflectance and h_N is the near-infrared diffuse attenuation coefficient, and for the visible, or PAR, wavelength interval where $p_1\rightarrow\gamma$ so that $A\rightarrow 0$,

$$\frac{da_v}{dL_t}\rightarrow A_v\rightarrow 0 \tag{20}$$

where a_v is the visible or PAR surface reflectance.

The results of equations (19) and (20) are important, as they indicate that for the dark-soil case the variation of surface reflectance with total leaf area index is primarily functional on the near-infrared spectral reflectance. We can extend this argument by

considering the variation of the simple ratio (SR) (i.e. NIR/red) and the normalized difference vegetation index (NDVI) (i.e. (NIR − red)/(NIR + red)) with the changing green-leaf area index. For this discussion, we redefine both of these terms as functions of reflectances rather than radiances to give

$$\mathrm{SR} = \frac{a_N}{a_v} \tag{21}$$

$$\mathrm{NDVI} = \frac{a_N - a_v}{a_N + a_v} \tag{22}$$

Differentiating the above expressions with respect to L_t and substituting in equations (19) and (20) gives us

$$\frac{d(SR)}{dL_t} \propto \exp(-2h_N L_t) \tag{23}$$

and

$$\frac{d(\mathrm{NDVI})}{dL_t} = \frac{da_N}{dL_t}\frac{2a_v}{(a_v + a_N)^2}$$

$$\propto \exp(-2h_N L_t)\frac{a_v}{(a_N + a_v)^2} \tag{24}$$

In the case of SR (equation (23)), the dependence of the near-infrared/visible signal combination on the NIR contribution is clear; with the NDVI (equation (24)), the dependence, while present, is complicated by the additional term, which includes a_N in the denominator (a_N varies with L_t). Generally speaking, however, the reflectance analogues of the SR and NDVI and their derivatives are functionally dependent on the $\exp(-2h_N L_t)$ term in the dark-soil case and the $\exp(-2h_v L_t)$ term when the soil is light (see Sellers 1986).

The biophysical functioning of individual leaves in the canopy has been shown to depend on the amount of PAR incident on their surfaces (under stress-free conditions). Now the expression for the attenuation of radiation down through the canopy is, from equation (14),

$$F_L = F_0\left(\frac{1 - h_4}{\sigma}\right)\exp(-KL) + h_5\exp(-hL) + h_6\exp(hL) \tag{25}$$

where F_0 is the PAR flux (in W/m) above the canopy and F_L is the PAR flux at level L in the canopy.

In the case of a canopy of horizontal leaves, this gives for the PAR flux

$$F_L \simeq F_0\exp(-h_v L_t) \tag{26}$$

where h_v is the attenuation coefficient for PAR.

If we ignore the contribution of reflected radiation from the soil surface, we can describe the total absorption of PAR by the canopy, IPAR, by

$$\mathrm{IPAR} = F_0(1 - a_v - \exp(-h_v L_t)) \tag{27}$$

in which case

$$\frac{d(\mathrm{IPAR})}{dL_t} = F_0 h_v \exp(-h_v L_t) \propto \exp(-h_v L_t) \tag{28}$$

Equation (28) is reasonable in that it shows a dependence of IPAR upon the one-way penetration of PAR down through the canopy.

Equation (26), which describes the attenuation of PAR within the canopy, may be inserted into the expressions for individual leaf photosynthesis and stomatal resistance, and the resultant functions integrated over the depth of the canopy to yield total canopy photosynthesis and resistance

$$P_c = \int_0^{L_t} P\,dL$$

$$= \int_0^{L_t} \frac{a_1 F_0 \exp(-h_v L_t)}{b_1 + F_0 \exp(-h_v L_t)} - R_d\,dL \tag{29}$$

where P_c is the canopy photosynthetic rate (in kg/m^2/s^1), and

$$\frac{1}{r_c} = \int_0^{L_t} \frac{1}{r_s} dL$$

$$= \int_0^{L_t} \left[\frac{a_2}{b_2 + F_0 \exp(-h_v L_t)} + c_2 \right]^{-1} dL \tag{30}$$

where r_c is the minimum canopy resistance (in s/m).

Solutions for the above expressions for P_c and r_c may be found in Sellers (1985) for a variety of leaf-angle distributions. Figure 6 illustrates the dependence of P_c and r_c on L_t and on each other: it is clear that if the near-linearity of the relationship between P and r_s holds for an individual leaf then it will translate to the full canopy situation. To obtain the incremental variation of P_c and r_c with total leaf-area index, L_t, it is merely necessary to differentiate equations (29) and (30) with respect to L_t and insert the upper limit of L_t, which gives

$$\frac{dP_c}{dL_t} = \frac{a_1 F_0 \exp(-h_v L_t)}{b_1 + F_0 \exp(-h_v L_t)} \tag{31}$$

$$\frac{d(1/r_c)}{dL_t} = \left[\frac{a_2}{b_2 + F_0 \exp(-h_v L_t)} + c_2 \right] \tag{32}$$

or, for small radiative fluxes

$$\frac{dP_c}{dL_t}, \frac{d(1/r_c)}{dL_t} \propto \exp(-h_v L_t) \tag{33}$$

Equation (33) shows that the variation of canopy photosynthesis and transpiration resistance are dependent upon the one-way penetration of PAR and hence are linearly related to IPAR for small radiative fluxes (see equation (28)). Equation (33) may be compared with the derivatives of SR and NDVI with L_t:

$$\frac{d(\mathrm{SR})}{dL_t}, \frac{d(\mathrm{NDVI})}{dL_t} \propto \exp(-2h_N L_t) \tag{34}$$

From the above we can see that the biophysical processes of canopy photosynthesis and stomatal resistance and the absorption of PAR are related to the exponential extinction of PAR by the coefficient h_v, which has the value of $(1 - w_v)^{1/2}$, and the total leaf-area index L_t. The remote-sensing indicators of chlorophyll density, SR and NDVI, are normally dependent upon the near-infrared canopy reflectance, which

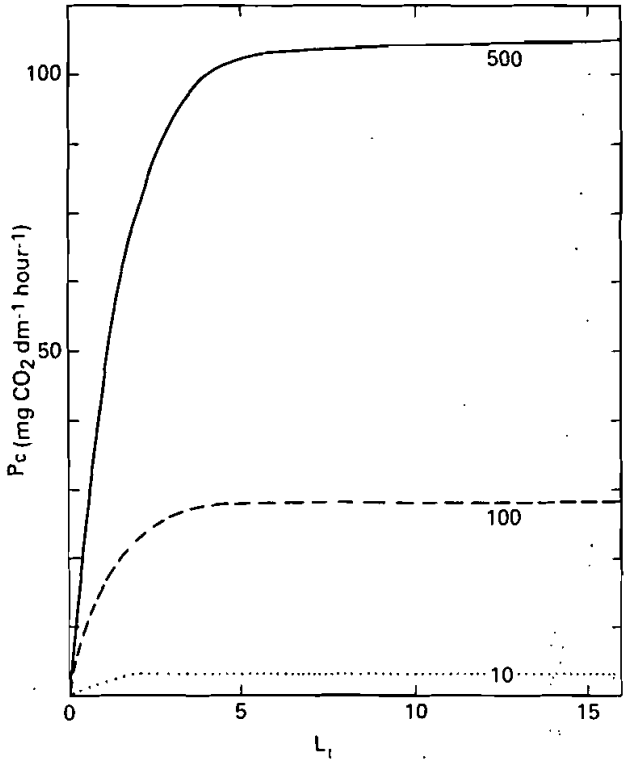
100
50
0
5
10
15
500
100
10
P_c (mg CO_2 dm^{-1} $hour^{-1}$)
L_t

(*a*)

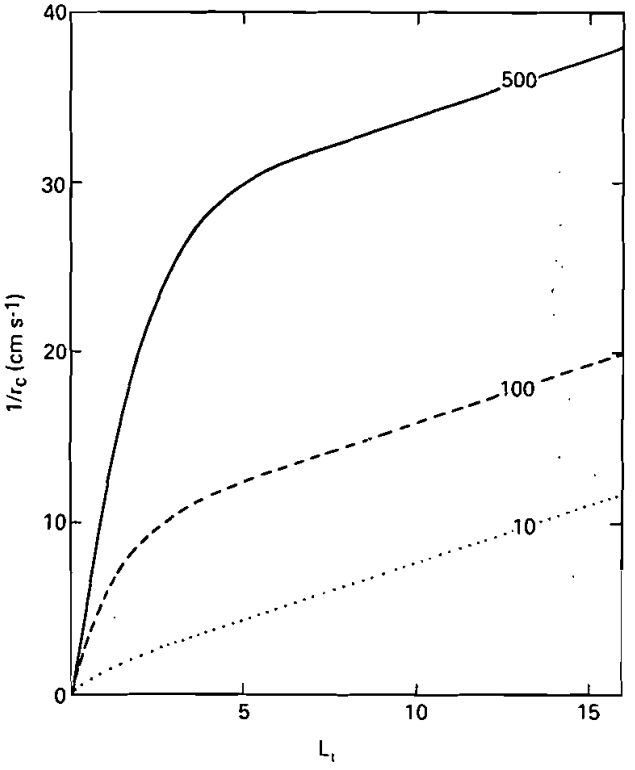
40
30
20
10
0
5
10
15
500
100
10
$1/r_c$ (cm s^{-1})
L_t

(*b*)

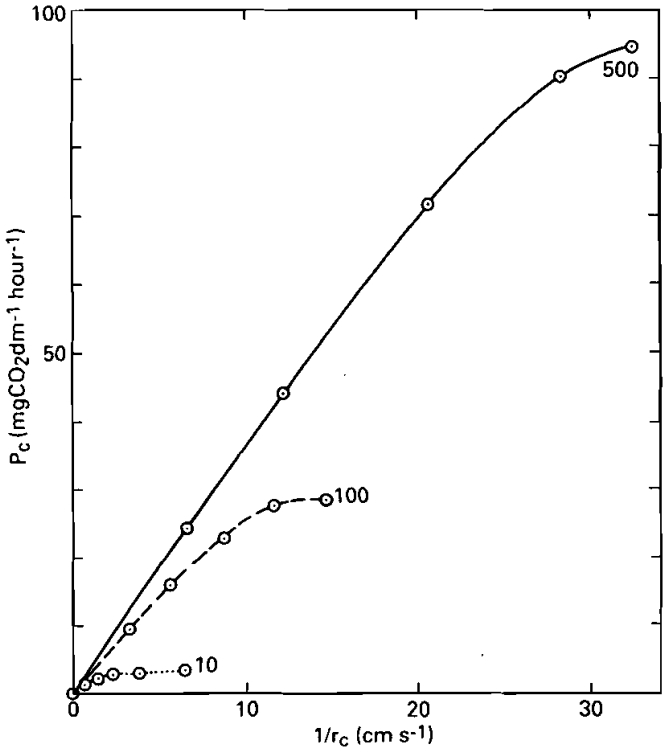

Figure 6. (*a*) Canopy photosynthesis (P_c) for a model maize canopy using the integral of leaf photosynthesis description, as a function of total leaf area index L_t. A range of responses to differing PAR levels is shown, and PAR fluxes are noted next to each curve in W/m^2. (*b*) Canopy inverse resistance ($1/r_c$) or conductance for a model maize canopy. (*c*) Canopy photosynthetic rate plotted against canopy conductance for the model maize canopy. The P_c and $1/r_c$ responses shown have been plotted against each other with the PAR intensities noted with the respective curves in W/m^2.

varies with the product of the near-infrared attenuation coefficient, h_N, which is equal to $(1-w_N)^{1/2}$. Both of these conclusions are based on simple integrations of individual leaf characteristics—reflectance, transmittance, photosynthetic and stomatal resistance responses to incident PAR—over whole canopies by the application of a simple radiative-transfer model.

5. Relations between canopy reflectance and biophysical properties

Finally, we can relate the biophysical and scattering properties of the plant canopy to each other. Using the SR as an example of a reflectance indicator (the following discussion is also pertinent to the NDVI), we can define the rate of change of our three biophysical variables—IPAR, P_c and r_c—as derivatives with respect to SR. To do this, we use the differentiation chain rule: the common variable L_t may be eliminated in

order to obtain expressions for the variation of P_c, r_c and IPAR with respect to SR:

$$\frac{d(\text{IPAR})}{dL_t}=\frac{d(\text{IPAR})}{dL_t}\left[\frac{d(\text{SR})}{dL_t}\right]^{-1}\propto\frac{\exp(-h_v L_t)}{\exp(-2h_N L_t)} \tag{35}$$

$$\frac{d(P_c)}{d(\text{SR})}=\frac{d(P_c)}{dL_t}\left[\frac{d(\text{SR})}{dL_t}\right]^{-1}\propto\frac{\exp(-h_v L_t)}{\exp(-2h_N L_t)} \tag{36}$$

$$\frac{d(1/r_c)}{d(\text{SR})}=\frac{d(1/r_c)}{dL_t}\left[\frac{d(\text{SR})}{dL_t}\right]^{-1}\propto\frac{\exp(-h_v L_t)}{\exp(-2h_N L_t)} \tag{37}$$

The results in equations (35)–(37) are crucial to the arguments presented here. They demonstrate that an increase in total leaf-area index L_t will increase the canopy photosynthesis and inverse resistance at a rate governed by the value $\exp(-h_v L_t)$ and the simple ratio by a rate governed by the value of $\exp(-2h_N L_t)$. From the above, we will have linear or near-linear relationships between the biophysical and reflectance properties of the surface if the right-hand sides of equation (35)–(37) are constant or nearly so for any value of L_t. In all these cases, this condition will only be met if

$$\exp(-2h_N L_t)=\exp(-h_v L_t)$$

or

$$2h_N L_t = h_v L_t$$

$$2(1-\omega_N)^{1/2}=(1-\omega_v)^{1/2}$$

$$\omega_N = 1-\tfrac{1}{4}(1-\omega_v) \tag{38}$$

If this condition is met exactly then P_c, $1/r_c$ and IPAR will be near-linearly related to SR and NDVI. If we use the idealized values of $\omega_v=0{\cdot}2$ and $\omega_N=0{\cdot}8$ then (38) is true. Dickinson (1983) reported broadband values for green leaves of $\omega_v=0{\cdot}165$ ($0{\cdot}3$–$0{\cdot}7\,\mu$m) and $\omega_N=0{\cdot}825$ ($0{\cdot}7$–$3{\cdot}0\,\mu$m), which comes fairly close to satisfying (38). Figure 7, reproduced from Sellers (1985), shows estimates of P_c and r_c plotted against SR and NDVI using the Dickinson (1983) values for ω_v and ω_N and values of $0{\cdot}15$ and $0{\cdot}3$ for the soil reflectance in the PAR and near-infrared wavelength intervals. Values of a_1, b_1, a_2, b_2 and c_2 are appropriate to maize leaves and may be found in Sellers (1985). It is clear that, even though the ω_v/ω_N combination of the Dickinson (1983) data is not the ideal one of (38), the relationship between the biophysical and reflectance properties of the canopy is near-linear. Also of interest in figure 7 is the effect of increasing leaf area index on both sets of properties: additional increments of leaf area index are seen to yield progressively smaller increases in SR, P_c and $1/r_c$. It is clear that the reduction is related to $\exp(-2h_N L_t)$ in the case of SR and NDVI and to $\exp(-h_v L_t)$ in the cases of P_c and $1/r_c$.

6. Summary and discussion

We should conclude this theoretical discussion with some reference to the real world. The remainder of this journal issue is dedicated primarily to specific field studies and the application of operational and non-optimal remote-sensing systems to infer the biophysical properties associated with natural vegetation, which is neither homogenous, randomly distributed not made up of horizontal isotropic leaves. It is useful to review the major limitations of our simple theoretical analysis presented here

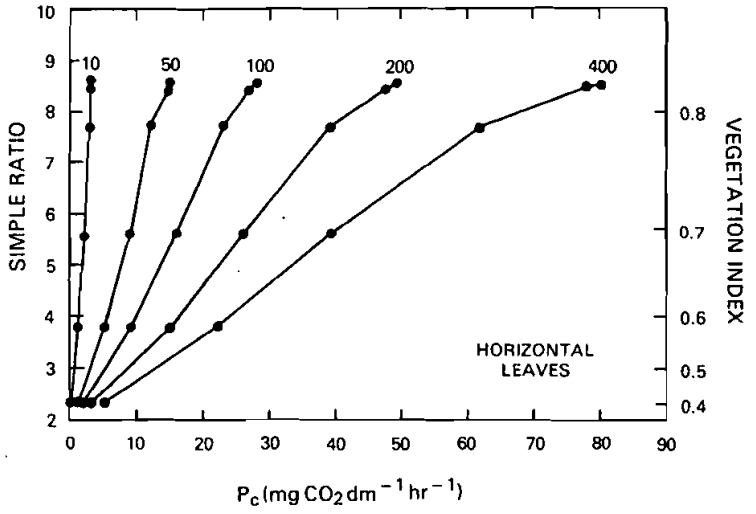

(*a*)

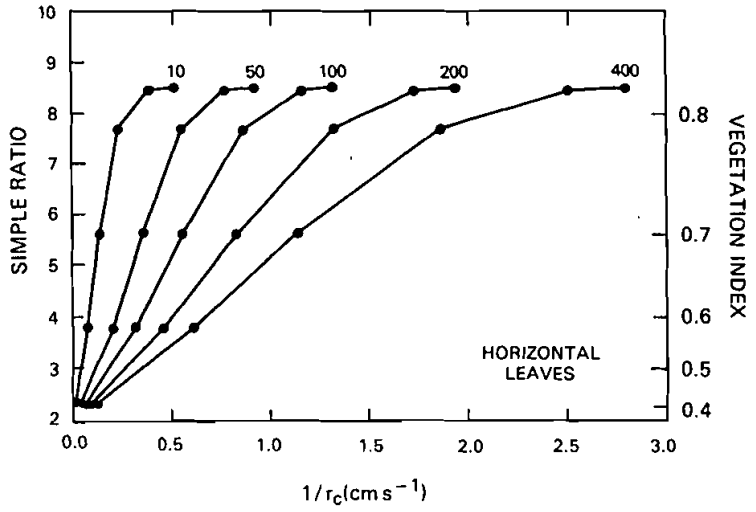

(*b*)

Figure 7. (*a*) Canopy photosynthetic rate for the model maize canopy plotted against the calculated NIR/red ratio and the NDVI as given by the two-stream approximation model. Increasing levels of PAR flux density are shown against the top curves in W/m^2. Solid circles on the lines correspond to leaf-area indices for 0·1, 0·5, 1·0, 2·0, 4·0 and 6·0 progressing from left to right. The crop is assumed to be a uniform green cover of maize with leaf and soil spectral properties specified in Sellers (1985). (*b*) Canopy conductance for the model maize canopy plotted against the calculated NIR/red ratio and the NDVI as given by the two-stream approximation. All other information is the same as in (*a*).

and to bear in mind that more complex realistic models will probably suffer from the same problems.

(i) Surface heterogeneity: almost all radiative-transfer models applied to vegetation assume that the canopy elements are randomly distributed over the horizontal plane. Clustered elements or sub-pixel-scale patches of bare ground may complicate the interpretation of multispectral data (see Sellers 1985).

(ii) Greenness: the presence of a fraction of dead leaves in the canopy would appear to reduce SR and NDVI to values approaching those typical of bare soils (see Sellers 1985, Harris 1986). However, many plant canopies shed dead leaves via abscission, and the extent to which the non-green leaf fraction is a problem needs to be determined from experimental studies.

(iii) Leaf orientation and solar zenith angle: the correlation of multispectral data with leaf area index is dependent on leaf orientation and solar elevation for canopies with non-horizontal leaf angle distribution functions.

(iv) View angle: operational measurements of surface reflectances are usually made with narrow-field-of-view sensors. More sophisticated radiative-transfer models must be used to describe the angular distribution of the reflected radiation above the surface.

With regard to the first three points, we can expect the relationships between reflectance and leaf area index to be severely affected. However, a reduction in the reflectance indicator also implies a similar reduction in P_c and $1/r_c$, so the data may still be applied to estimate vegetation biophysical properties (Sellers 1985).

In spite of the above and other problems, it is reasonable to assume that the SR and NDVI as provided by satellite systems should yield near-linear estimates of the area-averaged canopy photosynthetic capacity and minimum resistance. To use the reflectance data effectively for remotely sensed applications, other quantities must be estimated (PAR flux and the species dependent biophysical coefficients in equations (2) and (7)). This result supports the view that the reflectance data provide indications of the instantaneous biophysical rates associated with plant canopies; gross primary productivity and evapotranspiration, rather than reliable estimates of any state associated with the vegetation, such as leaf area index or biomass.

From the preceding discussion, it can be seen that the integral of NDVI with respect to time provides an estimate of gross primary production. To be comparable among different regions, this must be weighted by the respective PAR fluxes, losses such as respiration, and the efficiencies of the conversion process (Monteith 1977, Kumar and Monteith 1982, Steven *et al.* 1983). Comparisons within a given area for the same year or for the same area over several years for the same time period have been reported, and experimentally confirm the theory we have presented here. Our treatment of the NDVI and SR as being estimators of rate processes such as the photosynthetic capacity and evapotranspiration has been corroborated by Tucker *et al.* (1986), where globally averaged NDVI data were found to be inversely related to globally averaged relative atmospheric CO_2 measurements. Goward *et al.* (1985) reported a good agreement between North American NDVI time-integral data and published figures for ecosystem net primary production. Additional experimental confirmation of the meaning of the NDVI, SR and other 'greenness' measures comes from the experimental findings of Tucker *et al.* (1981) from ground-collected NDVI and SR time-integral data and the

destructively sampled total above-ground biomass production data from winter wheat. These same relationships have been extended to satellite data in a subsequent study over a three-year period where NOAA-7 AVHRR NDVI time-integral data were found to be similarly correlated with total herbaceous biomass production data from the Sahel zone in northern Senegal (Tucker *et al.* 1985). The companion papers in this issue report on other uses of satellite spectral data for studying various aspects of primary production from African environments.

References

ALLEN, W. A., GAUSMAN, H. W., and RICHARDSON, A. J., 1973, Willstatter–Stoll theory of leaf reflectance evaluated by ray tracing. *Appl. Optics*, **12**, 2448.

ALLEN, W. A., GAUSMAN, H. W., RICHARDSON, A. J., and CARDENAS, R., 1971, Water and air changes in grapefruit, corn, and cotton leaves with maturation. *Agron. J.*, **63**, 392.

ALLEN, W. A., GAUSMAN, H. W., RICHARDSON, A. J., and THOMAS, A. J., 1969, Interaction of isotropic light with a compact plant leaf. *J. opt. Soc. Am.*, **59**, 1376.

ALLEN, W. A., GAUSMAN, H. W., RICHARDSON, A. J., and WIEGAND, C. L., 1970, Mean effective optical constants of thirteen kinds of plant leaves. *Appl. Optics* **9**, 2573.

COLWELL, J. A., 1974, Vegetation canopy reflectance. *Remote Sensing Environ.*, **3**, 175.

CURRAN, P. J., 1983, Multispectral remote sensing for the estimation of green leaf area index, *Phil. Trans. R. Soc.* A, **309**, 257.

CURCIO, J. A., and PETTY, C. C., 1951, Extinction coefficients for pure liquid water. *J. opt. Soc. Am.*, **41**, 302.

DICKINSON, R. E., 1983, Land surface processes and climate-surface albedos and energy balance, *Adv. Geophys.*, **25**, 305.

DUGGIN, M. J., 1977, Likely effects of solar elevation on the quantification of changes in vegetation with maturity using sequential Landsat imagery. *Appl. Optics*, **16**, 521.

ELVIDGE, C. D., and *Lyon, R. J. P.*, 1985, Influence of rock-soil spectral variation on the assessment of green biomass. *Remote Sensing Environ.*, **17**, 265.

EZRA, C. E., TINNEY, L. R., and JACKSON, R. D., 1984, Effect of soil background on vegetation discrimination using Landsat data. *Remote Sensing Environ.*, **16**, 233.

FARQUHAR, G. D., AND SHARKEY, T. D., 1982, Stomatal conductance and photosynthesis. *A. Rev. Plant Physiol.*, **33**, 317.

FARQUHAR, G. D., and VON CAEMERRER, S., 1982, Modeling of photosynthetic response to environmental conditions, in *Encyclopedia of Plant Physiology*, Vol. 12B, edited by O. L. Lange, P. S. Noble, C. B. Osmond and H. Ziegler (Berlin, Heidelberg: Springer-Verlag), p. 549.

FRASER, R. S., and KAUFMAN, Y. F., 1985, The relative importance of aerosol scattering and absorption in remote sensing, *I.E.E.E. Trans. Geosci. remote Sensing*, **23**, 625.

GATES, D. M., KEEGAN, H. J., SCHLETER, J. C., and WEIDNER, V. P., 1965, Spectral properties of plants. *Appl. Optics*, **4**, 11.

GAUSMAN, H. W., 1974, Leaf reflectance of near-infrared. *Photogram. Engng*, **40**, 183.

GOWARD, S. A., TUCKER, C. J., and DYE, D., 1985. North American Vegetation patterns observed with the NOAA-7 Advanced Very High Resolution Radiometer. *Vegetatio*, **64**, 3.

HARRIS, R., 1986, Vegetation index models for the assessment of vegetation in marginal areas, *Int. J. remote Sensing* (submitted).

HESKETH, J. D., and BARKER, D., 1967, Light and carbon assimilation by plant communities. *Crop Sci.*, **7**, 285.

HOLBEN, B. N., 1986, Characteristics of maximum-value composite images from temporal AVHRR data. *Int. J. remote Sensing*, **7**, 1417.

HOLBEN, B. N., and FRASER, R. S., 1984, Red and near-infrared sensor response to off-nadir viewing, *Int. J. remote Sensing*, **5**, 145.

HUERTE, A. R., POST, D. F., and JACKSON, R. D., 1984, Soil spectral effects on 4-space vegetation discrimination. *Remote Sensing Environ.*, **15**, 155.

HEURTE, A. R., POST, D. F., and JACKSON, R. D., 1985, Spectral response of a plant canopy with different soil backgrounds. *Remote Sensing Environ.*, **17**, 37.

JACKSON, R. D., 1983, Spectral indices in *n*-space, *Remote Sensing Environ.*, **13**, 409.

JARVIS, P. G., 1976, The interpretation of the variations in leaf water potential and stomatal conductance found in canopies in the field. *Phil. Trans. R. Soc.* B, **273**, 593.

KIMES, D. S., 1983, Dynamics of directional reflectance factor distributions for vegetation canopies. *Appl. Optics*, **22**, 1364.

KIMES, D. S., 1984, Modeling the directional reflectance from complete homogeneous vegetation canopies with various leaf-orientation distributions, *J. opt. Soc. Am.* A, **1**, 725.

KIMES, D. S., HOLBEN, B. N., TUCKER, C. J., and NEWCOMB, W. W., 1984, Optimal directional view angles for remote-sensing missions. *Int. J. remote Sensing*, **5**, 887.

KIMES, D. S., SMITH, J. A., and RANSON, K. J., 1980, Vegetation reflectance measurements as a function of solar zenith angle, *Photogramm. Engng remote Sensing*, **46**, 1563.

KNIPLING, E. B., 1970, Physical and physiological basis for the reflectance of visible and near-infrared radiation from vegetation. *Remote Sensing Environ.*, **1**, 155.

KUMAR, M., and MONTIETH, J. L., 1982; Remote sensing of crop growth, In *Plants and the Daylight Spectrum*, edited by H. Smith (London: Academic Press), p. 134.

KUMAR, R., and SILVA, L., 1973, Light ray tracing through a leaf cross section. *Appl. Optics*, **12**, 2950.

MEADOR, W. E., and WEAVER, W. R., 1980, Two-stream approximations to radiative transfer in planetary atmospheres: a unified description of existing methods and a new improvement. *J. atmos. Sci.*, **37**, 630.

MONTEITH, J. L., 1977, Climate and the efficiency of crop production in Britain, *Phil. Trans. R. Soc.* B, **271**, 277.

PERRY, C. R., and LAUTENSCHLAGER, L. F., 1984, Functional equivalence of spectral vegetation indices. *Remote Sensing Environ.*, **14**, 169.

ROSS, J., 1975, Radiative transfer in plant communities. In *Vegetation and the Atmosphere*, Vol. I, edited by J. L. Monteith (London: Academic Press), p. 13.

SALISBURY, F. B., and ROSS, C., 1969, *Plant Physiology* (Belmont California: Wadsworth Press).

SELLERS, P. J., 1985, Canopy reflectance, photosynthesis and transpiration. *Int. J. remote Sensing*, **6**, 1335.

SELLERS, P. J., 1986, Canopy reflectance, photosynthesis, and transpiration II: The role of biophysics in the linearity of their interdependence. *Remote Sensing Environ.* (in the press).

STEVEN, M. D., BISCOE, P. V., and JAGGARD, K. W., 1983, Estimation of sugar beet productivity from reflection in the red and infrared spectral bands. *Int. J. remote Sensing*, **4**, 325.

TUCKER, C. J., 1978, A comparison of satellite sensor bands for monitoring vegetation, *Photogramm. Engng remote Sensing*, **44**, 1369.

TUCKER, C. J., 1980, Remote sensing of leaf water content in the near infrared. *Remote Sensing Environ.*, **10**, 23.

TUCKER, C. J., FUNG, I. Y., KEELING, C. D., and GAMMON, R. H., 1986, Relationship between atmospheric CO_2 variations and a satellite-derived vegetation index. *Nature, Lond.*, **319**, 195.

TUCKER, C. J., and GARRATT, M. W., 1977, Leaf optical system modeled as a stochastic process. *Appl. Optics*, **16**, 635.

TUCKER, C. J., HOLBEN, B. N., ELGIN, J. H., and MCMURTREY, J. E., 1981, Remote sensing of total dry matter accumulation in winter wheat. *Remote Sensing Environ.*, **13**, 461.

TUCKER, C. J., VANPRAET, C. L., SHARMAN, M. J., and VAN ITTERSUM, G., 1985, Satellite remote sensing of total herbaceous biomass production in the Senegalese Sahel: 1980–1984. *Remote Sens. Environ.*, **17**, 233.

TURNER, N. C., 1974, Stomatal response to light and water under field conditions, *R. Soc. N.Z. Bull.*, **12**, 423.

WILLIAMS, W. E., 1983, Optimal water-use efficiency in a California shrub. *Plant Cell Environ.*, **6**, 145.

WILLSTAETTER, A., and STOLL, K., 1918, *Untersuchungen über die Assimilation der Kohlensaure* (Berlin: Springer-Verlag), p. 122.

WOOLLEY, J. T., 1971, Reflectance and transmittance of light by leaves. *Plant Physiol.*, **47**, 656.